

Electrically controllable self-assembly for radial alignment of gold nanorods in liquid crystal droplets

Nan Wang,¹ Julian S. Evans,^{1,*} Qingkun Liu,² Shaowei Wang,¹ Iam-Choon Khoo,³ and Sailing He^{1,4}

¹Centre for Optical and Electromagnetic Research, Zhejiang Provincial Key Laboratory for Sensing Technologies, Zhejiang University, Hangzhou 310058, China

²Department of Physics, University of Colorado at Boulder, Boulder, CO 80309, USA

³Department of Electrical Engineering, Pennsylvania State University, University Park, PA 16802, USA

⁴Department of Electromagnetic Engineering, JORCEP, Royal Institute of Technology, S-100 44 Stockholm, Sweden
[*julian@coer-zju.org](mailto:julian@coer-zju.org)

Abstract: We demonstrate the dispersion and alignment of gold nanorods in 5CB liquid crystal droplets in silicon oil with a radial director structure. This biphasic system shows that the nanorods are stabilized against phase boundary driven aggregation. The radial alignment of the droplets can be further controlled by electric field. This method is potentially useful for the fabrication of hybrid nanostructured materials, such as plasmonic polymer dispersed liquid crystals and self-assembly-based devices; it could also be extended for use with magnetic, semi-conducting, or up-conversion nanoparticles.

©2015 Optical Society of America

OCIS codes: (160.4236) Nanomaterials; (160.3710) Liquid crystals; (250.5403) Plasmonics.

References and links

1. C. M. Soukoulis, S. Linden, and M. Wegener, "Negative refractive index at optical wavelengths," *Science* **315**(5808), 47–49 (2007).
2. V. M. Shalaev, "Optical negative-index metamaterials," *Nat. Photonics* **1**(1), 41–48 (2007).
3. J. Valentine, S. Zhang, T. Zentgraf, E. Ulin-Avila, D. A. Genov, G. Bartal, and X. Zhang, "Three-dimensional optical metamaterial with a negative refractive index," *Nature* **455**(7211), 376–379 (2008).
4. J. Yao, Z. Liu, Y. Liu, Y. Wang, C. Sun, G. Bartal, A. M. Stacy, and X. Zhang, "Optical negative refraction in bulk metamaterials of nanowires," *Science* **321**(5891), 930 (2008).
5. J. Tien, A. Terfort, and G. M. Whitesides, "Microfabrication through electrostatic self-assembly," *Langmuir* **13**(20), 5349–5355 (1997).
6. C. A. Mirkin, R. L. Letsinger, R. C. Mucic, and J. J. Storhoff, "A DNA-based method for rationally assembling nanoparticles into macroscopic materials," *Nature* **382**(6592), 607–609 (1996).
7. M. R. Jones, R. J. Macfarlane, B. Lee, J. Zhang, K. L. Young, A. J. Senesi, and C. A. Mirkin, "DNA-nanoparticle superlattices formed from anisotropic building blocks," *Nat. Mater.* **9**(11), 913–917 (2010).
8. R. J. Macfarlane, B. Lee, M. R. Jones, N. Harris, G. C. Schatz, and C. A. Mirkin, "Nanoparticle superlattice engineering with DNA," *Science* **334**(6053), 204–208 (2011).
9. P. Poulin, H. Stark, T. C. Lubensky, and D. A. Weitz, "Novel colloidal interactions in anisotropic fluids," *Science* **275**(5307), 1770–1773 (1997).
10. K. J. Stebe, E. Lewandowski, and M. Ghosh, "Materials science. Oriented assembly of metamaterials," *Science* **325**(5937), 159–160 (2009).
11. K. Hur, Y. Francescato, V. Giannini, S. A. Maier, R. G. Hennig, and U. Wiesner, "Three-Dimensionally Isotropic Negative Refractive Index Materials from Block Copolymer Self-Assembled Chiral Gyroid Networks," *Angew. Chem. Int. Ed. Engl.* **50**(50), 11985–11989 (2011).
12. G. Pawlik, K. Tarnowski, W. Walasik, A. C. Mitus, and I. C. Khoo, "Liquid crystal hyperbolic metamaterial for wide-angle negative-positive refraction and reflection," *Opt. Lett.* **39**(7), 1744–1747 (2014).
13. I. C. Khoo, A. Diaz, J. Liou, M. V. Stinger, J. Huang, and Y. Ma, "Liquid crystals tunable optical metamaterials," *IEEE J. Sel. Top. Quantum Electron.* **16**(2), 410–417 (2010).
14. I. C. Khoo, "Nonlinear optics, active plasmonics and metamaterials with liquid crystals," *Prog. Quantum Electron.* **38**(2), 77–117 (2014).
15. M. B. Ross, M. G. Blaber, and G. C. Schatz, "Using nanoscale and mesoscale anisotropy to engineer the optical response of three-dimensional plasmonic metamaterials," *Nat. Commun.* **5**, 4090 (2014).

16. Q. Liu, Y. Cui, D. Gardner, X. Li, S. He, and I. I. Smalyukh, "Self-alignment of plasmonic gold nanorods in reconfigurable anisotropic fluids for tunable bulk metamaterial applications," *Nano Lett.* **10**(4), 1347–1353 (2010).
17. H. K. Bisoyi and S. Kumar, "Liquid-crystal nanoscience: an emerging avenue of soft self-assembly," *Chem. Soc. Rev.* **40**(1), 306–319 (2011).
18. Q. Liu, N. Wang, P. Chen, Y. Zhang, and S. He, "Large-area bulk self-assembly of plasmonic nanorods in nematic liquid crystal via surface-mediated alignment," *Opt. Mater. Express* **3**(11), 1918–1924 (2013).
19. Q. Liu, Y. Yuan, and I. I. Smalyukh, "Electrically and Optically Tunable Plasmonic Guest-Host Liquid Crystals with Long-Range Ordered Nanoparticles," *Nano Lett.* **14**(7), 4071–4077 (2014).
20. S. Umadevi, X. Feng, and T. Hegmann, "Large Area Self-Assembly of Nematic Liquid-Crystal-Functionalized Gold Nanorods," *Adv. Funct. Mater.* **23**(11), 1393–1403 (2013).
21. D. F. Gardner, J. S. Evans, and I. I. Smalyukh, "Towards reconfigurable optical metamaterials: colloidal nanoparticle self-assembly and self-alignment in liquid crystals," *Mol. Cryst. Liq. Cryst. (Phila. Pa.)* **545**(1), 1227–1245 (2011).
22. J. Pérez-Juste, L. M. Liz-Marzan, S. Carnie, D. Y. C. Chan, and P. Mulvaney, "Electric-field-directed growth of gold nanorods in aqueous surfactant solutions," *Adv. Funct. Mater.* **14**(6), 571–579 (2004).
23. G. von Maltzahn, A. Centrone, J. H. Park, R. Ramanathan, M. J. Sailor, T. A. Hatton, and S. N. Bhatia, "SERS-coded gold nanorods as a multifunctional platform for densely multiplexed near-infrared imaging and photothermal heating," *Adv. Mater.* **21**(31), 3175–3180 (2009).
24. H. Wang, T. B. Huff, D. A. Zweifel, W. He, P. S. Low, A. Wei, and J. X. Cheng, "In vitro and in vivo two-photon luminescence imaging of single gold nanorods," *Proc. Natl. Acad. Sci. U.S.A.* **102**(44), 15752–15756 (2005).
25. T. Lee, R. P. Trivedi, and I. I. Smalyukh, "Multimodal nonlinear optical polarizing microscopy of long-range molecular order in liquid crystals," *Opt. Lett.* **35**(20), 3447–3449 (2010).
26. E. Brasselet, N. Murazawa, H. Misawa, and S. Juodkazis, "Optical vortices from liquid crystal droplets," *Phys. Rev. Lett.* **103**(10), 103903 (2009).
27. Y. Uchida, Y. Takahashi, and J. Yamamoto, "Controlled fabrication and photonic structure of cholesteric liquid crystalline shells," *Adv. Mater.* **25**(23), 3234–3237 (2013).
28. M. Humar and I. Musevic, "3D microlasers from self-assembled cholesteric liquid-crystal microdroplets," *Opt. Express* **18**(26), 26995–27003 (2010).
29. J. H. Noh, H. L. Liang, I. Drevensek-Olenik, and J. Lagerwall, "Tunable multicoloured patterns from photonic cross-communication between cholesteric liquid crystal droplets," *J. Mater. Chem. C* **2**(5), 806–810 (2014).
30. M. Humar, M. Ravnik, S. Pajk, and I. Musevic, "Electrically tunable liquid crystal optical microresonators," *Nat. Photonics* **3**(10), 595–600 (2009).

1. Introduction

Nanostructured materials are of great interest for their properties not found in naturally occurring materials. Preparation of nanostructured materials can be achieved in a "top-down" lithographic approach [1–4] or in a "bottom-up" self-assembly driven approach. Self-assembly allows relatively simple building-blocks to achieve complex architectures through electrostatic [5], DNA-mediated [6–8], and elastic interactions [9], as demonstrated in plasmonic nano-structures for optical metamaterials [10–15] and polarization components [15]. Owing to their unique ability to exert inter-molecular reorienting torque and their fluid (but correlated) natures [9], liquid crystals (LC) are excellent hosts for self-assemblies of nanoparticles [16]. Various ordered phases of liquid crystals are also highly susceptible to electric field, magnetic field or other external stimuli [17–19] to enable tunability in the resulting properties of the nano-structured devices. Recently, the Hegmann and Smalyukh groups have demonstrated self-assembly of gold nanoparticles in nematic 4-cyano-4'-pentylbiphenyl (5CB) with silica [20] and polyethylene glycol [19] coatings respectively. However, the Frank elastic energy associated with colloidal inclusions in LC made achieving a stable dispersion challenging as phase barriers have surface tension that can cause nanoparticles to aggregate [21].

Here we demonstrate a biphasic system with nematic 5CB droplets in silicon oil with gold nanorods (GNRs) well dispersed (concentration is less than 0.8 wt%) and aligned into a radial structure. The alignment of GNRs can be further controlled by electric field. The aligned GNRs show strong polarization and wavelength dependent transmission. Polarizing optical microscopy (POM) and polarizing multi-photon excitation fluorescence microscopy were used to characterize the alignment of LC and GNRs. This method is potentially useful for the

fabrication of hybrid nanostructured materials and self-assembly-based devices; it could also be extended for use with magnetic, semi-conducting, or up-conversion nanoparticles.

2. Experiment

Aqueous dispersions of cetyl trimethylammonium bromide (CTAB)-capped GNRs with a mean diameter of 20 nm and a mean length of 50 nm were synthesized by a seed-mediated method [22]. The dispersion of GNRs was centrifuged at 9000 rpm for 10 min twice and then re-dispersed into 1 mL of deionized water. To functionalize and stabilize the GNRs [23], 3 mg of 5kDa Thiol-terminated methoxy-poly(ethylene glycol) (mPEG-SH, JemKem Technology) dissolved in 1 ml of water was added into 15 mL of GNR dispersions with optical density of 0.6 (length of the sample measured is 10 mm). The mixture was set overnight and was then purified via centrifugation at 9000 rpm for 10 min to eliminate the excess mPEG-SH. The recapping procedure was repeated to ensure a complete removal of the CTAB from the GNRs. The GNRs were then centrifuged at 9000 rpm for 10 min and re-suspended into 1mL of methanol. After that, the methanol was fully evaporated from the 1 mL of GNR dispersions and the dry GNRs left were added into 20 μ L of 5 CB (from Chengzhi Yonghua Display Materials Co. Ltd.) The mixture was heated to 40°C and sonicated for 5 min, until the GNRs were well dispersed into isotropic 5CB. Then the mixture was cooled down and vigorously stirred while 5CB turned into the nematic phase. Stirring should only be performed at temperatures which are a few degrees under the clear point of 5CB, when the elastic constants are low, otherwise stirring will cause the GNRs to aggregate. The GNR-LC composites were centrifuged at 2400 rpm for 2.5 min to remove GNR aggregates [19]. Finally, 5 μ L of GNR-LC composites and 100 μ L of silicon oil were mixed and stirred slightly to form GNRs-dispersed LC droplets to allow for the observation of large isolated droplets. Since the densities of 5CB LC and silicon oil are similar, the GNRs-dispersed LC droplets in silicon oil are stable for the duration of the experiment.

The LC cell was made of two pieces of glass with transparent indium tin oxide electrodes on their inner surfaces. The LC cell filled with GNRs-dispersed LC droplets in silicon oil is 160 μ m thick to allow for the observation of large (diameter~100 μ m) droplets which have strong colors with relatively dilute concentrations of GNRs. A sinusoidal electric voltage with maximum value V_{\max} 12V and frequency 1 kHz was applied to the LC cell by an electronic oscillator when the behavior of GNRs-dispersed LC droplets in electric field was examined.

POM and polarizing multi-photon excitation fluorescence microscopy were adopted to characterize the alignment of LC and GNRs. A femtosecond Ti:Sapphire laser (Mira HP, Coherent,) with a pulse duration time of 150 fs and a repetition rate of 80 MHz was used to generate the multi-photon excitation fluorescence from gold nanorods and liquid crystal. The laser beam was directed into an Olympus microscope (FV1000) by a 20 \times objective (NA = 0.75) to focus the laser beam onto the sample and the signal was detected by a photomultiplier tube.

3. Results and discussion

The GNRs-dispersed LC droplets in silicon oil were characterized by POM and transmission optical microscopy. The transmission optical microscopy with incident light linearly polarized reveals the images of a GNRs-dispersed LC droplet as Figs. 1(a) and 1(b) (corresponding to two orthogonal polarization of incident light respectively). The POM texture of GNRs-dispersed LC droplets (Fig. 1(c)) shows the characteristic 4 fringed dark cross whose two arms are parallel to the polarizations of analyzer and polarizer respectively indicative of a strength 1 defect. Further investigation on the LC droplets by polarizing multi-photon excitation fluorescence microscopy confirms that the alignment of LC is radial (schematically shown in Fig. 1(d)).

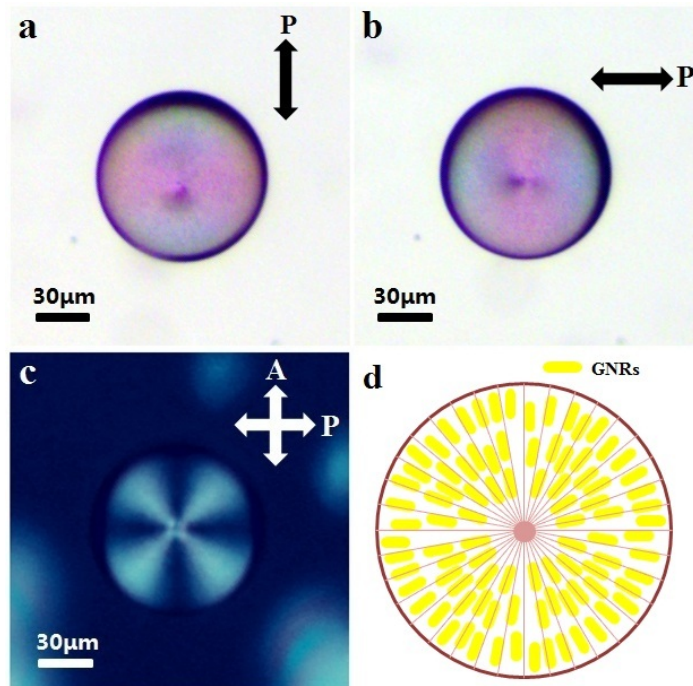


Fig. 1. (a), (b) The transmission optical microscopy images of a GNRs-dispersed LC droplet in silicon oil with a linearly polarized incident light ((a) and (b) correspond to two orthogonal polarizations of incident light). The thickness of the LC cell is 160 μm . P indicates the polarization of the incident light. (c) POM textures of the GNRs-dispersed LC droplets. P and A indicate the polarizations of the polarizer and analyzer. (d) Schematic illustration of GNRs alignment in a LC droplet. The solid lines indicate the director field of the LC.

Since GNRs are aligned in the LC matrix, the collective surface plasmon resonance (SPR) is excited and the droplet shows strong polarization and wavelength dependent transmission. When the long axis of GNRs is parallel to the polarization of incident light, the longitudinal SPR mode is excited and the light with wavelength of 680 nm was strongly absorbed and scattered by the GNRs. In contrast, when the long axis of GNRs is perpendicular to the polarization of incident light, the transverse SPR mode is excited and light with a wavelength of 530 nm is absorbed and scattered. In the green areas of the droplet, which have strong extinction of 680 nm light, the long axes of GNRs have a preferential direction parallel to the polarization of incident light. While in the red areas, the long axes of GNRs have a preferential direction perpendicular to the polarization of incident light.

The overall configurations of LC and GNRs in a LC droplet in silicon oil are illustrated in Fig. 1(d). LC and GNRs all follow radial alignment in the droplet, which is consistent with the tangential boundary conditions observed in reference [19]. Furthermore, the GNRs were only observed in LC droplets and not found in silicon oil; we attribute this to the fact that the GNRs are highly stable in the LC and not chemically compatible with the silicon oil.

GNRs-dispersed LC droplets with smaller diameters in silicon oil were also characterized by polarizing multi-photon excitation fluorescence microscopy. The multi-photon excitation fluorescence signal of the GNRs-dispersed LC droplets with excitation at 850 nm and detection within 495–540 nm (Fig. 2(a)) shows the two-photon luminescence (TPL) of the GNRs with spectra characterized in Ref [24]. TPL shows strong polarization-dependence as a $\cos^4\theta$ (θ is the angle between long axis of GNR and the polarization of incident light) function [24]. The polarization dependent intensity of the signal reveals that the GNRs follow radial alignment.

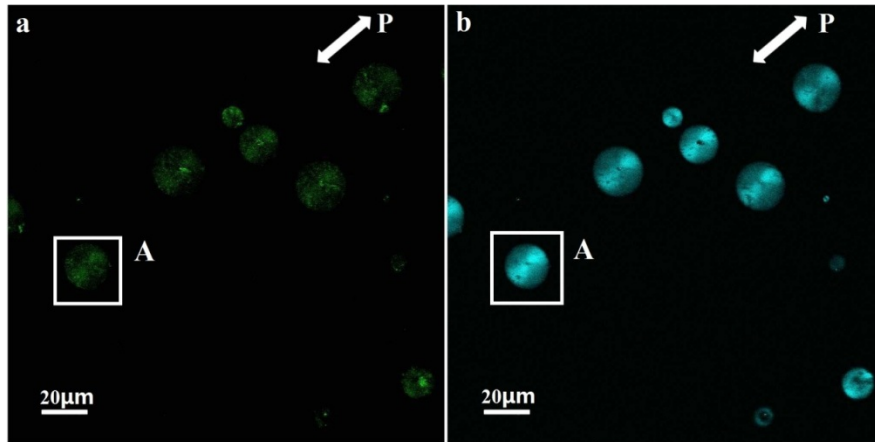


Fig. 2. (a) Polarizing two-photon excitation fluorescence microscopy image of the GNRs self-assembled in LC droplets with excitation at 850 nm and detection within 495–540 nm. P indicates the polarization of the excitation light. (b) Polarizing three-photon excitation fluorescence microscopy image of the GNRs-dispersed LC droplets with excitation at 850 nm and detection within 420–460 nm.

The multi-photon excitation fluorescence signal of the GNRs-dispersed LC droplets with excitation at 850 nm and detection within 420–460 nm (Fig. 2(b)) is the superposition of the three-photon excitation fluorescence (3PF) of 5CB with spectra characterized in Ref [25], and the TPL of the GNRs. 3PF of 5CB is also highly polarization dependent and follows a $\cos^6\theta$ (θ is the angle between the director of LC and the polarization of incident light) function [25]. Since the signal of the GNRs is much weaker than that of 5CB and can be neglected, the polarization dependent signal in Fig. 2(b) reveals the radial alignment of the LC. Even though Figs. 2(a) and 2(b) only demonstrate one cross section near the equatorial plane of droplet A, however the images of each layer obtained by polarizing multi-photon excitation fluorescence microscopy all verify the configuration of GNRs and LC illustrated in Fig. 1(d).

The alignment of LC and GNRs in the droplets can be controlled by electric field. A sinusoidal electric voltage with its maximum value of 12 V and frequency of 1 kHz is added to the 160 μm thick LC cell. The LC has positive dielectric anisotropy and tends to align with the electric field. Moreover, the GNRs are self-assembled by the LC and the transmission optical microscopy images of the GNRs-dispersed LC droplets (Figs. 3(a), 3(b)) show most of the area change to red, which suggests that the transverse SPR mode of the GNRs is excited and the long axis of the GNRs have a preferential direction parallel to the electric field. Only the fringes of the LC droplet still show some longitudinal SPR mode, which is the result of the boundary conditions imposed on the LC by silicon oil. Generally, the alignment of GNRs and LC are controlled by the electric field and the overall configurations of the GNRs and the LC are illustrated in Fig. 3(d). The POM texture of the LC droplet in the electric field (Fig. 3(c)) shows a faint ring which is associated with the $s = 1/2$ disclination loop on the “sheaf of wheat” configuration schematically shown in Fig. 3(d). The switching time of the GNRs-dispersed droplets visually appears to be on the order of a few seconds.

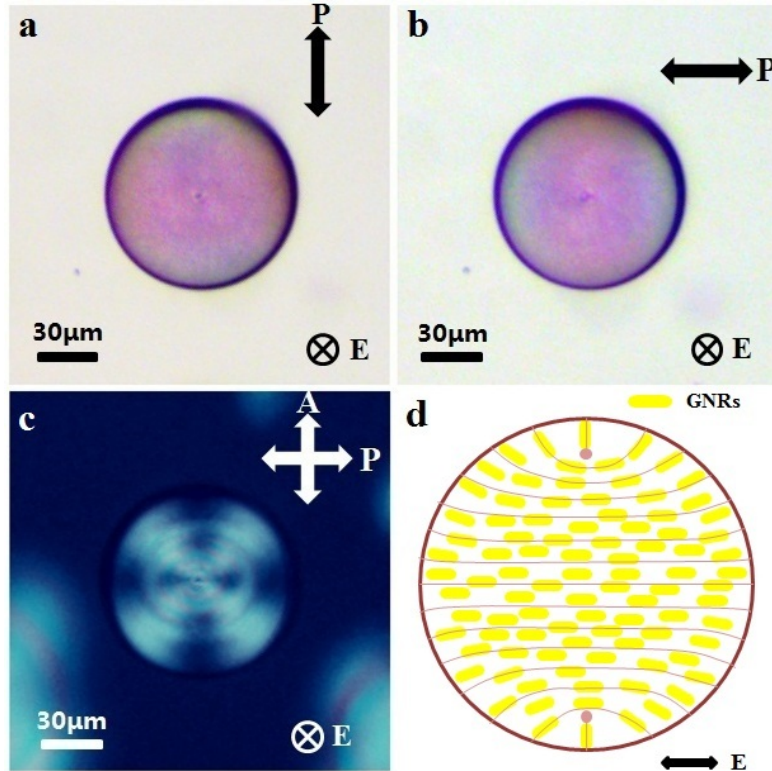


Fig. 3. (a), (b) The transmission optical microscopy images of the GNRs-dispersed LC droplets with sinusoidal electric voltage (V_{\max} is 12V and frequency is 1kHz) added to the cell (thickness is 160 μm). The incident light is linearly polarized and P indicates the polarization of the incident light. (E) indicates the direction of the electric field. (c) POM textures of the GNRs-dispersed LC droplets in the same electric field. (d) Schematic illustration of GNRs alignment (XZ cross section) in a LC droplet set in an electric field. The red lines indicate the director field of the LC. The red dots indicate the disclination line.

4. Conclusions

In this work, we have achieved radial alignment of GNRs in a sphere with the help of LC droplets in silicon oil. The alignment of GNRs can be further controlled by electric field. The aligned GNRs show strong polarization and wavelength dependent transmission. The electrically controllable radial alignment of colloidal GNRs has been achieved for the first time. This method can be improved by using polymer-stabilized LC to enhance the stability of the system and further extended by adopting different phases of LC. By using different structures to align GNRs in various forms, this approach will enable a new class of hybrid nanostructured materials and self-assembly-based devices, such as tunable microantennae, LC-droplet-based optical vortex generators [26], omnidirectional lasing modes [27–29], and microresonator cavities [30] whose properties can also be modified by a rich array of nanoparticles.

Acknowledgments

We thank Yaoran Sun and Jianwei Tang for useful discussions. This research was supported by the National Natural Science Foundation of China (Nos. 91233208 and 61178062) and the Program of Zhejiang Leading Team of Science and Technology Innovation, Swedish VR grant (# 621-2011-4620) and AOARD. Professor I. C. Khoo acknowledges the support from Sir Pao Yu-Kong Chair Professorship during his visit to Zhejiang University.